VIP Ammonia Decomposition Very Important Paper

DOI: 10.1002/anie.201410773

# Lithium Imide Synergy with 3d Transition-Metal Nitrides Leading to Unprecedented Catalytic Activities for Ammonia Decomposition**

*Jianping Guo, Peikun Wang, Guotao Wu, Anan Wu, Daqiang Hu, Zhitao Xiong, Junhu Wang, Pei Yu, Fei Chang, Zheng Chen, and Ping Chen**

***Abstract:*** *Alkali metals have been widely employed as catalyst promoters; however, the promoting mechanism remains essentially unclear. Li, when in the imide form, is shown to synergize with 3d transition metals or their nitrides TM(N) spreading from Ti to Cu, leading to universal and unprecedentedly high catalytic activities in $NH_3$ decomposition, among which $Li_2NH$–MnN has an activity superior to that of the highly active Ru/carbon nanotube catalyst. The catalysis is fulfilled via the two-step cycle comprising: 1) the reaction of $Li_2NH$ and 3d TM(N) to form ternary nitride of LiTMN and $H_2$, and 2) the ammoniation of LiTMN to $Li_2NH$, TM(N) and $N_2$ resulting in the neat reaction of $2\,NH_3 \rightleftharpoons N_2 + 3\,H_2$. $Li_2NH$, as an $NH_3$ transmitting agent, favors the formation of higher N-content intermediate (LiTMN), where Li executes inductive effect to stabilize the TM–N bonding and thus alters the reaction energetics.*

With more than a hundred years of research and development, heterogeneous catalysis has accumulated enormous experimental and theoretical data that allow the correlation, in principle, of the electronic structure of a catalyst with the rate of an elementary step involved in a catalytic process, which lays the foundation of a catalyst genome.[1] The data base, however, has a weak link in the concrete and systematic description of the nature of electronic promoters, the substances that play vital roles in enhancing activity, selectivity, and/or stability of catalysts for numerous processes including ammonia and Fischer–Tropsch syntheses, water-gas shift, hydrocarbon dehydrogenation, and so on.[2] The difficulties in elucidating the properties of electronic promoters mainly lie in the facts that they are normally present in small quantities and the lack of in situ structural information.[3] It is, therefore, not a surprise to note that the continuous efforts in identifying the chemical state of K and its interaction with Fe or Ru in ammonia synthesis, as an example, has lasted for decades.[2] In-depth surface science and theoretical investigations show that K may decrease the work function of transition metals and enhance the dissociative adsorption of $N_2$ by electron donation to Fe or Ru,[4] and/or weaken the chemisorption of $NH_3$ by electrostatic interactions.[5] $K_2O$, KOH, and a K-O-Fe species have been proposed as the chemical forms.[6] The unclear chemical nature is also true for other alkali metals, although the promoting capability has been found to be in the order Cs > K > Na > Li.[7] Herein we employ $NH_3$ decomposition, a chemical process that has been extensively studied for understanding the fundamentals of $NH_3$ synthesis for over half a century and is attracting increasing attentions to be a potential route providing $CO_x$-free hydrogen for fuel cells in recent years,[8] as a reference reaction, and choose Li, commonly regarded as the least electron donating alkali, as a promoter to illustrate that the elusive electronic-promoting effect can be elucidated when Li is in imide form and the intermediate ternary nitride species of Li and transition-metal is formed. More importantly, such an understanding paves the way for catalytic materials design and development for processes of chemical production and clean energy harvesting.

Catalysts developed for $NH_3$ decomposition are mainly based on Group 8 transition metals, among which Ru has the highest activity followed by Ir, Rh, Ni, and Fe.[9] Early 3d transition metals, namely Ti, V, Cr, and Mn, form stable nitrides under an $NH_3$ atmosphere and are essentially inactive towards $NH_3$ decomposition under moderate conditions.[10] Such a situation changes drastically when $Li_2NH$ takes part in. It should be put forth here that, to focus on the neat interaction between 3d transition metal and $Li_2NH$ and to facilitate the related characterizations, a high content of $Li_2NH$ was employed in this study.

Metallic Li reacts with $NH_3$ to form $LiNH_2$, which decomposes to $NH_3$ and $Li_2NH$, a compound with cubic structure and with high Li ion mobility and capability in storing hydrogen,[11] at temperatures above 523 K under a flow of argon. An incidental finding that led us to the present study is the substantial amount of $H_2$ and $N_2$ co-produced with $NH_3$ when $LiNH_2$ was tested in a stainless steel rather than a quartz reactor (Supporting Information, Fig-

[*] J. Guo, P. Wang, Prof. Dr. G. Wu, D. Hu, Prof. Dr. Z. Xiong, Prof. Dr. J. Wang, P. Yu, F. Chang, Prof. Dr. P. Chen
Collaborative Innovation Center of Chemistry for Energy Materials, State Key Laboratory of Catalysis
Dalian Institute of Chemical Physics
Chinese Academy of Sciences, Dalian 116023 (P. R. China)
E-mail: pchen@dicp.ac.cn
Homepage: http://www.imide.dicp.ac.cn
Prof. Dr. A. Wu, Z. Chen
State Key Laboratory of Physical Chemistry of Solid Surfaces and College of Chemistry and Chemical Engineering
Xiamen University, Xiamen 361005 (P. R. China)

[**] This work was supported by the Project of National Natural Science Funds for Distinguished Young Scholars (51225206), 973 Project (2010CB631304), and the National Natural Science Foundation of China (21133004 and 21273187). We thank D. H. Gregory (University of Glasgow) for the discussions on ternary nitrides of Li and transition metals and H. Wu (NIST) and M. Yang (DICP) for sharing the information on metal nitrides and oxynitrides, and also the Shanghai Synchrotron Radiation Facility for providing the beam time.

Supporting information for this article is available on the WWW under http://dx.doi.org/10.1002/anie.201410773.

  

ure S1a,b). If purposely impregnating Fe on $LiNH_2$, significantly enhanced yields of $H_2$ and $N_2$ together with a large depression of $NH_3$ were observed showing considerable conversion of $NH_3$ to $N_2$ and $H_2$ (Supporting Information, Figure S1c).

Under a flow of pure $NH_3$, the $LiNH_2$-Fe sample shows catalytic activity at 623 K, which is about 100 K lower than that of $Fe_2N$ or Fe/CNTs. Its activity is over one order of magnitude greater than those of $Fe_2N$ and Fe/CNTs at temperatures below 723 K (Figure 1), manifesting the prominent promoting role of Li.

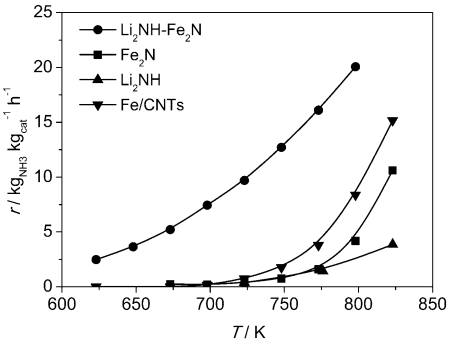


***Figure 1.*** Rates of ammonia decomposition catalyzed by the $Li_2NH$ and Fe-based samples. Reaction conditions: 30 mg catalyst, $NH_3$ flow rate 30 mL min$^{-1}$.

$Fe_2N$ and $Li_2NH$ were detected by XRD and XANES on a sample collected at 723 K (Figure 2b, Supporting Information, Figure S9). Neat $Li_2NH$ has a limited activity at temperatures below 773 K (Figure 1; Supporting Information, Figure S2), as does $Fe_2N$. A synergy between these two compounds may occur leading to the abnormally high catalytic activity, which can be demonstrated, to some extent, by the following experimental facts. First, the TPD-MS, XRD, and XANES measurements show that $Fe_2N$ reacts with $Li_2NH$ at temperatures above 500 K, giving rise to $H_2$ and $Li_3FeN_2$ according to the reaction R1 (Figure 2a and b). Removing $NH_3$ from the reacting system described in Figure 1 leads the formation of $Li_3FeN_2$ as well. Second, $Li_3FeN_2$ can be easily ammoniated to a mixture containing $LiNH_2$ and an amorphous Fe-containing compound (in which Fe remains in a tetrahedral coordination, Figure 2b and Supporting Information, Figure S3a) at ambient temperature. The mixture decomposes to $N_2$ and $NH_3$ at ca. 350 K and 500 K, respectively, regenerating $Fe_2N$ and $Li_2NH$ following the overall reaction R2 (Figure 2a and S3b). At elevated temperatures (see 500 K or above), the ammoniation of $Li_3FeN_2$ should give off $N_2$, $Fe_2N$ and $Li_2NH$ simultaneously. $Fe_2N$ and $Li_2NH$, again, go back to the R1 (Supporting Information, Figure S3c) creating a catalytic cycle that leads to the neat reaction R3:

$$3\,Li_2NH + Fe_2N \rightleftharpoons 2\,Li_3FeN_2 + 3/2\,H_2 \quad (R1)$$

$$2\,Li_3FeN_2 + NH_3 \rightleftharpoons 3\,Li_2NH + Fe_2N + 1/2\,N_2 \quad (R2)$$

$$NH_3 \rightleftharpoons 1/2\,N_2 + 3/2\,H_2 \quad (R3)$$

With $Li_3FeN_2$ as the starting chemical, similar activity was observed as that of $Li_2NH$-$Fe_2N$ (Supporting Information, Figure S4). The active phases are again $Fe_2N$ and $Li_2NH$. Third, $ND_3$ and $^{15}NH_3$ isotopic labeling characterizations on the $Li_2NH$-$Fe_2N$ and 5 wt% Ru/CNTs samples, respectively, carried out by performing steady-state isotopic transient kinetic analysis (SSITKA)[12] at 553 K, show that significantly more $^1H_2$ and $^{14}N_2$ are observable in the $Li_2NH$-$Fe_2N$ than in the Ru/CNTs within the first 5 min of gas shifting, and these additional $^1H_2$ and $^{14}N_2$ should have higher chances to form directly from the catalyst revealing the occurrences of the R1 and R2 under the reaction condition (indeed, both R1 and R2 can take place at lower or similar temperatures as compared with that of $NH_3$ decomposition over the $Li_2NH$-$Fe_2N$ as

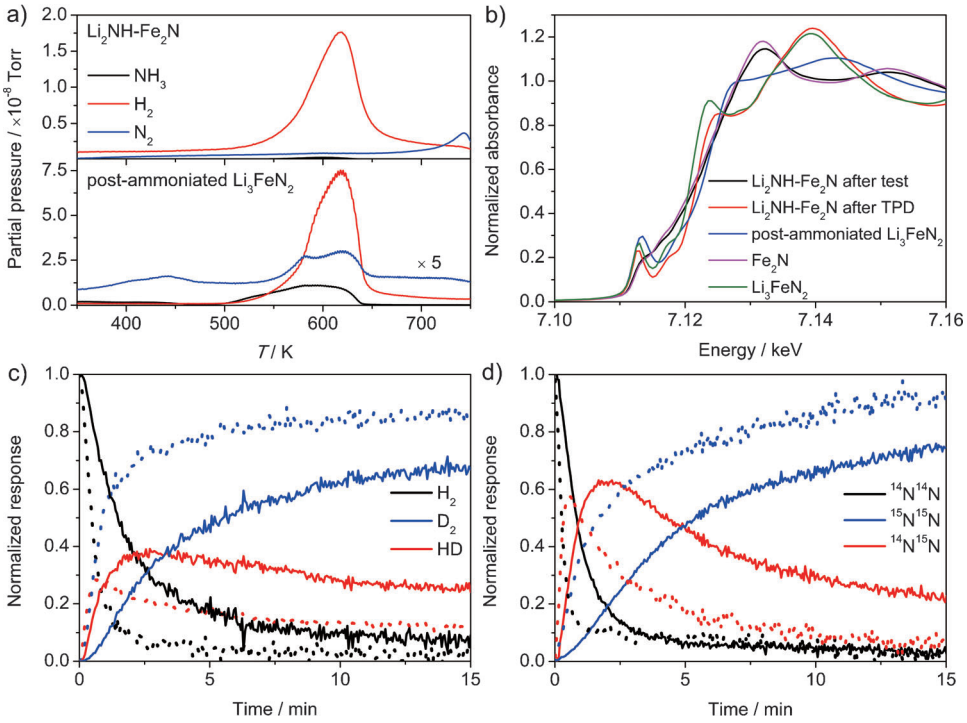


***Figure 2.*** Interactions of $Li_2NH$ and $Fe_2N$. a) TPD-MS signals of $H_2$, $N_2$ and $NH_3$ from the $Li_2NH$-$Fe_2N$ and post-ammoniated $Li_3FeN_2$ samples, respectively. b) Fe K-edge XANES spectra of the Fe-containing samples collected under different conditions. c), d) SSITKA analyses of the $Li_2NH$-$Fe_2N$ (——) and 5 wt% Ru/CNTs (•••••) samples under a gas shift from $NH_3$ to $ND_3$ and $^{14}NH_3$ to $^{15}NH_3$ at 553 K, respectively. Gas shifting was conducted at time = 0 min, the flow rate of 5 vol.% $NH_3$/Ar is 30 mL min$^{-1}$.

shown in Figure 1, Figure 2a; Supporting Information, Figure S3). HD and $^{14}N^{15}N$ overweigh $D_2$ and $^{15}N_2$ for a longer period time and remain in the outlet gas stream in the testing history of the $Li_2NH$-$Fe_2N$ as compared to that of the Ru/CNTs, reflecting continuous contributions of $^1H$ and $^{14}N$ from the catalyst to the gaseous products (Figure 2c and d) and also showing the likelihood of the involvement of bulk phase of the catalyst in the catalysis. Fourth, DFT calculations on the Fe-doped $Li_2NH$ system also indicate that the formation of $H_2$ is through the H transfer from N to Li nearby, which is "excited" by the interaction of Fe and N forming a Fe-N-Li moiety, followed by H–H coupling between H(N) and H(Li) (Supporting Information, Figure S5).

It should be pointed out that Li in $Li_2NH$ and $Li_3FeN_2$ are highly mobile[11a,13] under the reaction condition applied here; the reacting depth of catalyst particles in this particular case, as indicated by the SSITKA measurements, may be significantly greater than that of the conventional transition-metal-catalyzed process where the related catalysis occurs mainly on the top surface.

Fe has a few nitride forms $FeN_x$ ($0 < x \leq 1$), however, the N-rich nitride (FeN) is thermally unstable. The difficulty in dehydrogenation of $NH_3$ on Fe (100) surface, as simulated recently, increases with the increase in the surface N content owing to the insufficient Fe coordination to the $NH_x$ ($x = 0$, 1, and 2) intermediates,[14] in agreement with the low catalytic activity of neat Fe nitrides observed previously[10] and in this study. $Li_2NH$, repeatedly consumed and regenerated by R1 and R2, is beyond the role of electronic promoter. It is an $NH_3$ transmitting agent with activated N–H bonding (the N–H stretch at ca. 3160 $cm^{-1}$ for $Li_2NH$ vs. 3340 $cm^{-1}$ for $NH_3$). More importantly, Li, as the second cation to N, executes a positive inductive effect[15] to enhance the covalent Fe–N bonding, resulting in the significantly stabilized N-rich intermediate (that is, $Li_3FeN_2$, compositionally equivalent to $Li_3N + FeN$). Implied by the Brønsted–Evans–Polanyi (BEP) relationship, a reduced kinetic barrier and faster rate of reaction are expected, which is strongly supported by the abnormally high catalytic activity and low apparent activation energy of $Li_2NH$-$Fe_2N$ compared with neat $Fe_2N$ (Figure 1; Supporting Information, Figure S6).

Such an understanding leads us to establish a novel catalyst system for $NH_3$ decomposition, that is, 3d transition metals have a variety of stable or unstable interstitial lower N-content nitrides (TM(N) for short). They also have relatively stable higher N-content ternary nitrides with Li (LiTMN, except Zn).[16] Following the same catalytic cycle as that of $Li_2NH$-$Fe_2N$, the $Li_2NH$-3d TM(N) are expected to exhibit catalytic activities overweighing the neat 3d TM(N) in $NH_3$ decomposition.

The performances of $Li_2NH$-TM(N) spreading from Ti to Cu are shown in Figure 3a. The general catalytic features are as follows: 1) Universal catalytic activity. All $Li_2NH$-TM(N) tested here exhibit catalytic activities towards $NH_3$ decomposition at temperatures above 623 K, marking the drastic changes of the inert or low active neat TM(N) especially for the early 3d TM(N) and Cu[10,17] (Figure 3b; Supporting Information, Figure S7). 2) Unprecedentedly high activity. The hourly conversion of $NH_3$ per kg of catalyst at 773 K are ca. 1.9 kg for Ti-, 5.1 kg for V-, 15.7 kg for Cr-, 26.7 kg for Mn-, 16.1 kg for Fe-, 17.0 kg for Co-, 12.1 kg for Ni-, and 3.1 kg for Cu-$Li_2NH$ catalysts. Except for the $Li_2NH$-Ni (which is comparable to the Ni/SBA-15[18]), others are, to the best of our knowledge, the highest values achieved on the respective TM-based catalysts reported to date. We would like also to emphasize that, although the optimization to respective catalyst has yet to be carried out, the CrN-, $Fe_2N$-, MnN-,

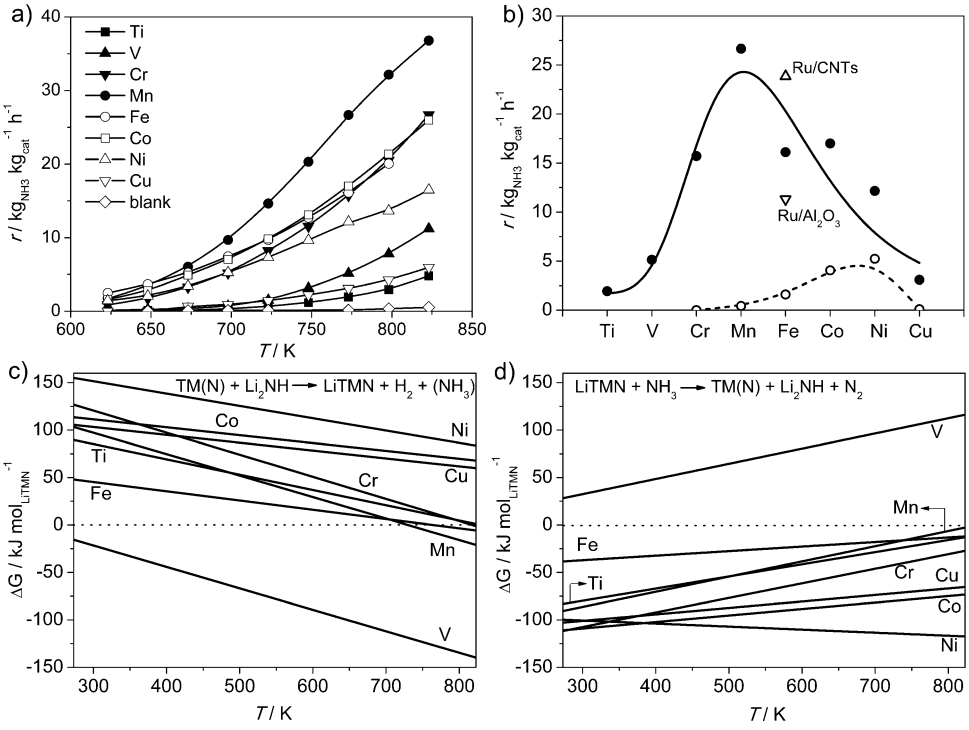


***Figure 3.*** Catalytic activities and thermodynamic analyses of the $Li_2NH$-TM(N). a) Catalytic activities of the $Li_2NH$-TM(N) samples, reaction condition is the same as that mentioned in Figure 1. b) Hourly $NH_3$ conversion at 773 K for the $Li_2NH$-TM(N) (●) vs. those of early 3d TMN and CNTs-supported Co, Ni, Cu (○) and Ru (△). Activity of 5 wt% $Ru/Al_2O_3$ (▽) is taken from Ref. [19]. c), d) Temperature dependence of the Gibbs free energy changes of the reactions 1) $TM(N) + Li_2NH \rightarrow LiTMN + H_2 + (NH_3)$ and 2) $LiTMN + NH_3 \rightarrow Li_2NH + TM(N) + N_2$.

  

and Co-$Li_2NH$ have activities significantly higher than that of 5 wt % $Ru/Al_2O_3$.[19] The $Li_2NH$-MnN is even superior to the highly active 5 wt % Ru/CNTs in the whole testing history. The overall catalytic activities of the $Li_2NH$-TM(N) exhibit a volcano shape centered at Mn site, in contrast to the neat 3d TM(N) where Ni was found to have the best performance (Figure 3b), such an interesting phenomenon is worthy of experimental and theoretical elucidation.[20] 3) Low operation temperature. Ti-, V-, and Cu-$Li_2NH$ catalysts exhibit activities at ca. 673 K, others at temperatures just above 623 K, representing the lowest starting temperatures reported for the respective metal-based catalysts. All these features evidence the significantly reduced kinetic barriers with the help of $Li_2NH$.

The TM to $Li_2NH$ weight ratio is kept at about 0.9 to allow the substantial formation of LiTMN to facilitate the characterization. Noted that the content of $Li_2NH$ can be largely reduced to a few weight percentage of TM(N) without causing substantial decrease in catalytic activity. Detailed characterizations and optimizations on the respective $Li_2NH$-TM(N) catalysts will be given in separated investigations. The general observations are that the catalytic cycle described for the $Li_2NH$-$Fe_2N$ is essentially kept by other $Li_2NH$-TM(N), that is, TM(N) reacts with $Li_2NH$ giving rise to $H_2$ and LiTMN, namely $Li_5TiN_3$, $Li_7VN_4$, $Li_9CrN_5$, $Li_7MnN_4$, $Li_{2.5}Co_{0.5}N$, LiNiN, and $Li_{2.5}Cu_{0.5}N$ ($NH_3$ is co-produced in some cases) following the reaction of $TM(N) + Li_2NH \rightarrow LiTMN + H_2 + (NH_3)$, where the easiness of $H_2$ release decreases essentially from Ti to Cu (Supporting Information, Figure S8). LiTMN, on the other hand, can be ammoniated to liberate $N_2$ according to the reaction of $LiTMN + NH_3 \rightarrow Li_2NH + TM(N) + N_2$, where the rates of ammoniation, on the contrary, are much slower for the early TMs (Supporting Information, Figure S10). The active state of 3d TM under the reaction condition is TiN, $Li_7VN_4$, CrN, MnN, $Fe_2N$, Co, Ni, or Cu, respectively (Supporting Information, Figure S9). The presence of active phases depends on the thermodynamic natures of the above two reactions. Based on the enthalpies of formation of $Li_2NH$, $NH_3$, and those reported binary and ternary nitrides,[21] and by counting the entropy of the gas only (unknown entropies of some nitrides), the temperature dependence of the Gibbs free energy changes per LiTMN of the corresponding two reactions are plotted in Figure 3c and d. The presence of TM(N) and $Li_2NH$ are thermodynamically favored at lower temperatures or high $NH_3$ partial pressures for most 3d TM except V, while LiTMN is favored at higher temperatures or under low $H_2$ or $NH_3$ partial pressures, in agreement with the experimental findings. Figure 3c and d also indicate that, within the accuracy of thermodynamic data, both the R1 and R2 have chances to take place under the reaction condition applied in this study.

The stabilization effect of alkali metals on the formation of oxides, oxynitrides, nitrides, and hydrides of TM of unusually high oxidation state is well known.[15,22] Coincidentally, O, N, and H etc. are common surface-rich species in many catalytic processes. It is, therefore, rational to extend our understanding on Li in promoting $NH_3$ decomposition to other catalytic processes. Indeed, a few recent investigations implied or proposed similar functionality of alkali metals in Fischer–Tropsch synthesis[23] and water-gas shift reaction.[24] In this context, a map linking the TM catalyst, the promoter A in proper chemical form and the reactive species X of an elementary reaction may be built up by searching combination of TM, A, and X that is relatively stable than [TM-X] by experimental trials and/or high-throughput computational materials design.[25] We would like to further emphasize that the endeavor in elucidating the promoting effect of alkali metals or alkaline earth metals on transition metal-based heterogeneous catalysis would benefit the materials development for energy harvesting, where the thermodynamic stability, the electronic structure, and the reactivity of respective material can be tuned by the involvement of alkali or alkaline earth metals. As pointed out in Ref. [22a], the forming compounds with alkali or alkaline earth metals favors the formation of a number of new TMO and TMON, the potential candidates for photocatalysis. In hydrogen production from thermochemical cycle, on the other hand, the important role of Na in tuning the thermodynamic properties of the cycle via stabilizing the higher O-content oxide of Mn has also been demonstrated.[26]

## Experimental Section

$Li_2NH$-3d TM(N) and TM(N) species were prepared by ball-milling the mixtures of transition-metal chlorides and $LiNH_2$ at 323 K, followed by washing and heating to 573 K in an argon flow. LiTMN compounds were prepared by calcining $Li_3N$ and respective metals under $N_2$ pressure at 923 K. The ammoniation of ternary lithium nitrides was performed in a homemade stainless steel reactor filled with pressurized $NH_3$. The structures of $Li_2NH$-TM(N) and LiTMN were characterized by XRD or XANES. Ammonia decomposition reaction was performed in a continuous-flow fixed-bed quartz reactor. The gas composition was analyzed using on-line gas chromatograph (GC-2014C, Shimadzu) equipped with a Porapak N column and TCD detector. Temperature-programmed reaction and SSITKA were employed to investigate the interactions between TM(N) and $Li_2NH$. See the Supporting Information for more detailed information.

Received: November 5, 2014
Published online: January 21, 2015

**Keywords:** ammonia decomposition · electronic promoter · heterogeneous catalysis · lithium imide · nitrides

[1] J. K. Nørskov, T. Bligaard, *Angew. Chem. Int. Ed.* **2013**, *52*, 776 – 777; *Angew. Chem.* **2013**, *125*, 806 – 807.
[2] B. E. Koel, J. Kim in *Handbook of Heterogeneous Catalysis* (Eds.: G. Ertl, H. Knözinger, F. Schüth, J. Weitkamp), Wiley-VCH, Weinheim, **2008**, pp. 1593 – 1624.
[3] T. W. Hansen, J. B. Wagner, P. L. Hansen, S. Dahl, H. Topsøe, C. J. H. Jacobsen, *Science* **2001**, *294*, 1508 – 1510.
[4] G. Ertl, M. Weiss, S. B. Lee, *Chem. Phys. Lett.* **1979**, *60*, 391 – 394.
[5] a) D. R. Strongin, G. A. Somorjai, *J. Catal.* **1988**, *109*, 51 – 60; b) S. Dahl, A. Logadottir, C. J. H. Jacobsen, J. K. Nørskov, *Appl. Catal. A* **2001**, *222*, 19 – 29.
[6] Z. Paál, G. Ertl, S. B. Lee, *Appl. Surf. Sci.* **1981**, *8*, 231 – 249.
[7] K. Aika, T. Takano, S. Murata, *J. Catal.* **1992**, *136*, 126 – 140.
[8] a) R. Z. Sørensen, J. S. Hummelshøj, A. Klerke, J. B. Reves, T. Vegge, J. K. Nørskov, C. H. Christensen, *J. Am. Chem. Soc.* **2008**,

  

*130*, 8660 – 8668; b) F. Schüth, R. Palkovits, R. Schlögl, D. S. Su, *Energy Environ. Sci.* **2012**, *5*, 6278 – 6289.
[9] a) S. F. Yin, B. Q. Xu, X. P. Zhou, C. T. Au, *Appl. Catal. A* **2004**, *277*, 1 – 9; b) F. Hayashi, Y. Toda, Y. Kanie, M. Kitano, Y. Inoue, T. Yokoyama, M. Hara, H. Hosono, *Chem. Sci.* **2013**, *4*, 3124 – 3130; c) A. H. Lu, J. J. Nitz, M. Comotti, C. Weidenthaler, K. Schlichte, C. W. Lehmann, O. Terasaki, F. Schüth, *J. Am. Chem. Soc.* **2010**, *132*, 14152 – 14162.
[10] C. R. Lotz, F. Sebba, *Trans. Faraday Soc.* **1957**, *53*, 1246 – 1252.
[11] a) B. A. Boukamp, R. A. Huggins, *Phys. Lett. A* **1979**, *72*, 464 – 466; b) P. Chen, Z. T. Xiong, J. Z. Luo, J. Y. Lin, K. L. Tan, *Nature* **2002**, *420*, 302 – 304.
[12] S. L. Shannon, J. G. Goodwin, *Chem. Rev.* **1995**, *95*, 677 – 695.
[13] M. Nishijima, Y. Takeda, N. Imanishi, O. Yamamoto, M. Takano, *J. Solid State Chem.* **1994**, *113*, 205 – 210.
[14] S. C. Yeo, S. S. Han, H. M. Lee, *J. Phys. Chem. C* **2014**, *118*, 5309 – 5316.
[15] J. Etourneau, J. Portier, F. Menil, *J. Alloys Compd.* **1992**, *188*, 1 – 7.
[16] N. Tapia-Ruiz, M. Segales, D. H. Gregory, *Coord. Chem. Rev.* **2013**, *257*, 1978 – 2014.
[17] A. Boisen, S. Dahl, J. K. Nørskov, C. H. Christensen, *J. Catal.* **2005**, *230*, 309 – 312.
[18] H. C. Liu, H. Wang, J. G. Shen, Y. Sun, Z. M. Liu, *Appl. Catal. A* **2008**, *337*, 138 – 147.
[19] S. F. Yin, B. Q. Xu, W. X. Zhu, C. F. Ng, X. P. Zhou, C. T. Au, *Catal. Today* **2004**, *93*, 27 – 38.
[20] A. Logadottir, T. H. Rod, J. K. Nørskov, B. Hammer, S. Dahl, C. J. H. Jacobsen, *J. Catal.* **2001**, *197*, 229 – 231.
[21] J. F. Herbst, L. G. Hector, Jr., *Phys. Rev. B* **2012**, *85*, 195137.
[22] a) Y. B. Wu, P. Lazic, G. Hautier, K. Persson, G. Ceder, *Energy Environ. Sci.* **2013**, *6*, 157 – 168; b) K. Miwa, S. Takagi, M. Matsuo, S. Orimo, *J. Phys. Chem. C* **2013**, *117*, 8014 – 8019.
[23] a) J. Gaube, H. F. Klein, *Appl. Catal. A* **2008**, *350*, 126 – 132; b) M. C. Ribeiro, G. Jacobs, B. H. Davis, D. C. Cronauer, A. J. Kropf, C. L. Marshaw, *J. Phys. Chem. C* **2010**, *114*, 7895 – 7903.
[24] Y. P. Zhai, D. Pierre, R. Si, W. L. Deng, P. Ferrin, A. U. Nilekar, G. W. Peng, J. A. Herron, D. C. Bell, H. Saltsburg, M. Mavrikakis, M. Flytzani-Stephanopoulos, *Science* **2010**, *329*, 1633 – 1636.
[25] S. Curtarolo, G. L. W. Hart, M. B. Nardelli, N. Mingo, S. Sanvito, O. Levy, *Nat. Mater.* **2013**, *12*, 191 – 201.
[26] B. J. Xu, Y. Bhawe, M. E. Davis, *Proc. Natl. Acad. Sci. USA* **2012**, *109*, 9260 – 9264.

  